Variability of Black Carbon mass concentration in surface snow at Svalbard

Michele Bertò[1#], David Cappelletti[2,7], Elena Barbaro[1,3], Cristiano Varin[1], Jean-Charles Gallet[4], Krzysztof Markowicz[5], Anna Rozwadowska[6], Mauro Mazzola[7], Stefano Crocchianti[2], Luisa Poto[1,3], Paolo Laj[8], Carlo Barbante[1,3] and Andrea Spolaor[1,2*].

[1]Ca' Foscari University of Venice, Dept. Environmental Sciences, Informatics and Statistics, via Torino, 155 - 30172 Venice-Mestre, Italy;
[2]Università degli Studi di Perugia, Dipartimento di Chimica, Biologia e Biotecnologie, Perugia, Italy;
[3]CNR-ISP, Institute of Polar Science – National Research Council –via Torino, 155 - 30172 Venice-Mestre, Italy;
[4]Norwegian Polar Institute, Tromsø, Norway.
[5]University of Warsaw, Institute of Geophysics, Warsaw, Poland;
[6]Institute of Oceanology, Polish Academy of Sciences, Sopot, Poland;
[7]CNR-ISP, Institute of Polar Science – National Research Council – Via Gobetti 101, Bologna;
[8]Univ. Grenoble-Alpes, CNRS, IRD, Grenoble-INP, IGE, 38000 Grenoble, France

[#] Now at Laboratory of Atmospheric Chemistry, Paul Scherrer Institute, 5232 Villigen PSI, Switzerland

Correspond to: Andrea Spolaor, andrea.spolaor@cnr.it; Michele Bertò, michele.berto@gmail.it

Abstract

Black Carbon (BC) is a significant forcing agent in the Arctic, but substantial uncertainty remains to quantify its climate effects due to the complexity of the different mechanisms involved, in particular related to processes in the snowpack after deposition. In this study, we provide detailed and unique information on the evolution and variability of BC content in the upper surface snow layer during the spring period in Svalbard (Ny-Ålesund). Two different snow-sampling strategies were adopted during spring 2014 and 2015, providing the *refractory* BC (rBC) mass concentration variability on a seasonal/daily and daily/hourly time scales. The present work aims to identify which atmospheric variables could interact and modify the mass concentration of BC in the upper snowpack, the snow layer which BC particles affects the snow albedo. Atmospheric, meteorological, and snow-related physical-chemical parameters were considered in a multiple linear regression model to identify the factors that could explain the variations of BC mass concentrations during the observation period. Precipitation

events were the main drivers of the BC variability. Snow metamorphism and activation of local sources during the snow melting periods appeared to play a non-negligible role (wind resuspension in specific Arctic areas where coal mines were present). The statistical analysis suggests that the BC content in the snow is not directly associated to the atmospheric BC load.

1. Introduction

In the last two decades, the Arctic region has been exposed to dramatic changes in terms of atmospheric temperature rise, sea ice decrease, and increase of air mass transport from lower latitudes bringing warmer and humid air masses containing pollutants and anthropogenic derived compounds (Law and Stohl, 2007; Comiso et al., 2008; Screen and Simmonds, 2010; Eckhardt et al., 2013; Schmale et al., 2018; Maturilli et al., 2019). Long-range transport and local emissions of combustion generating aerosols like black carbon (BC) can influence the radiative budget of the Arctic atmosphere, especially the impacts of atmospheric aging on the mixing state of BC particles (Eleftheriadis et al., 2009; Bond et al., 2013; Zanatta et al., 2018). When deposited over snow, numerous aerosol species directly increase the quantity of solar radiation absorbed by the snowpack, thus favouring snow aging processes and the decrease of the snow albedo (Hansen and Nazarenko, 2004; Flanner et al., 2007; Hadley and Kirchstetter, 2012; Skiles et al., 2018; Skiles and Painter, 2019).

Among these light-absorbing aerosols, *black carbon* (BC) particles are the most effective in absorbing the visible and near infrared solar radiation. These primarily emitted, insoluble, refractory and carbonaceous particles originate from natural and anthropogenic sources such as open fires or diesel engine exhausts. Currently, the anthropogenic emissions are higher compared to the natural ones (Moosmüller et al., 2009; Bond et al., 2013). In 2000, the energy production sector (including fossil fuels and solid residential fuels combustion) generated approximately 59% of the total global BC emissions while the remaining came from biomass burning (Bond et al., 2013). BC particles are characterized by a mass size distribution peaking around 100-250 nm (or mass equivalent diameter), e.g. 240 nm in the Svalbard area in spring (Bond et al., 2013; Laborde et al., 2013; Zanatta et al., 2016; Motos et al., 2019). The impact of BC particles absorbing the incoming solar radiation has indeed a non-negligible role in the Arctic region, which is already threatened by a two-fold temperature increase compared to the mid-latitude areas, the so-called "Arctic Amplification" (Bond et al., 2013; Cohen et al., 2014; Serreze and Barry, 2011). BC has an atmospheric lifetime of about seven days and has been directly targeted in important international mitigation agreements (AMAP, 2015). Theoretical and experimental results showed that the cryosphere is affected both by the BC-induced warming of the atmosphere and by direct and indirect BC effects on the snow once deposited over it (Flanner, 2013),

Atmospheric BC measurements in the Arctic regions are still rare, despite an extraordinary effort done by the international scientific community to evaluate the sources, transport paths, concentration, and climate impact (Eleftheriadis et al., 2009; Pedersen et al., 2015; Ferrero et al., 2016; Ruppel et al., 2017; Osmont et al., 2018; Zanatta et al., 2018; Laj et al., 2020). BC mass concentrations can be directly measured by using incandescent or thermal techniques and indirectly, by absorption measurements using an appropriate mass absorption cross-section (Petzold, 2013). Various terms such as refractory black carbon (rBC) for incandescent measurements, elemental carbon (EC) using thermal techniques, or equivalent black carbon (eBC) based on optical technique are used. Forsström et al. (2009) reported measurements performed in Arctic snow in the past and new measurements of EC in snow surface using filters and a thermo-optical method. The geographical and seasonal eBC variability was investigated in the Arctic region by Doherty et al. (2010). Other BC measurement in snow samples from the Arctic region can be found in Aamaas et al. (2011), Forsström et al. (2013), Pedersen et al. (2015), Gogoi et al. (2016), Khan et al. (2017) and Mori et al. (2019). Intercomparison of different techniques agree within a factor of 2 uncertainty at Alert (Sharma et al., 2017), Ny-Ålesund, and Barrow (Sinha et al., 2017).

A complex combination of processes are involved in the BC particles transfer from the atmosphere to the surface snow. Via a modelling approach, Liu et al. (2011) found that approximately 50% of BC's total burden in the Arctic atmosphere is removed through wet deposition-related processes. Yasunari et al. (2013) estimated the intensity of BC dry deposition on the Himalayan glaciers; they found that the surface roughness and the surface wind speed are critical parameters in order to retrieve realistic results. In a recent study, Jacobi et al. (2019) confirmed the previous estimates suggesting that approximately 60% of the BC particles are deposited on the surface snow via wet deposition in spring in the Svalbard Arctic area. Models are still not fully able to describe the actual deposition and transport processes in Svalbard, resulting in underestimating the BC concentration in the snowpack (Eckhardt, S. et al 2015, Stohl, A. et al. 2013). Although wet deposition is suggested to be the main driver of BC concentration in the snow, little is known about other environmental processes potentially affecting the BC particles concentration once deposited, i.e. physical post-depositional processes.

In this study we present two unique experiments performed in a clean area close to the town of Ny-Ålesund (Svalbard) at the Gruvebadet Aerosol Laboratory (78.91734 N, 11.89535 E, 40 m a.s.l.), during spring 2014 and 2015. Daily and hourly time resolution samplings were performed on the snow surface to investigate which atmospheric variables could directly or indirectly modify the BC mass concentration in the surface snow once deposited. The daily sampling lasted for approximately 85 days to assess the intra-seasonal variability covering the transition from a cold period (April) to the melting period in late June. The hourly time resolution experiment was performed to investigate the existence of potential processes affecting the BC concentration over the diurnal cycle.

2. Experimental Methods

2.1 Study Area

Both experiments were conducted in the proximity of the Ny-Ålesund research station (78.5526 N, 11.5519 E, 25 m a.s.l.), located on the Spitzbergen Island in Svalbard archipelago. Along the west coast, Svalbard is characterized by a maritime climate with an annual average temperature of -3.9°C in Ny-Ålesund (between 1994 and 2017) (Maturilli et al., 2019). On average, the snowpack starts building up in September and melts away at the end of May (Førland et al. 2011). Ny-Ålesund has become one of the reference locations for conducting Arctic climate studies focusing on atmospheric composition and physics. Long-term monitoring of atmospheric aerosols is performed at the Gruvebadet station (Feltracco et al., 2019, 2020, 2021a, 2021b; Moroni et al., 2018; Ferrero et al., 2016; Bazzano et al., 2015; Moroni et al., 2015; Zangrando et al., 2013; Scalabrin et al., 2012, Turetta er al., 2021), and at the Zeppelin observatory (475 m a.s.l.) (Eleftheriadis et al., 2009; Tunved et al., 2013; Lupi et al., 2016, and reference therein).

2.2 Snow Sampling

There are no standardized methods for sampling, filtering and analytical protocols for detecting atmospheric carbon deposited in snow, even if a few protocols have been developed (Ingersoll et al., 2009; Gallet et al., 2018; Meinander et al., 2020). In the present work, two different sampling strategies were adopted regarding the thickness of the sampled layer and the temporal sampling frequency.

Snow samples were collected during two field campaigns: The first campaign was carried out in Spring 2014, from April 1st to June 24th for a total of 85 days, it consists of daily sampling and it is referred hereafter as the "85-days experiment". The second campaign was conducted in Spring 2015 from April 28th to May 1st. During these three days, measurements were collected with hourly sampling. This second campaign is hereafter referred as the "3-days experiment". Snow samples were collected about 1 km North-West of Ny-Ålesund (Figure 1). The area is a dedicated clean site for aerosols and snow sampling, with no fuel engine traffic. The wind at the site is usually blowing from east to west, and rarely from North to South, minimizing the emission of the town reaching the sampling area. The main wind pattern during the experiment is presented in Figures 1 and 2. The samples for both experiments were kept frozen until the lab analyses. The samples were collected using neck nylon gloves to avoid any contamination.

The two experiments aim to capture the rBC mass concentration on a daily basis in the surface snow (upper 10 cm) during the seasonal change and on an hourly basis on a thinner surface snow layer (upper 3 cm) during a daily cycle. Although wet and dry deposition are the main sources of BC in the

Artic snow, the aim of our experiments was to evaluate if other atmospheric parameters could contribute to the snow surface rBC mass concentration variability.

In the 85-days experiment, the first 10 cm of surface snow were collected on a daily basis (approximately at 11.00 am, GMT+2) in the same area, using a 5 cm diameter and 10 cm long Teflon tube. The samples were collected following a straight line leaving about 15 cm between the sampling points to minimize the spatial variability. The collected snow was homogenized in a pre-cleaned plastic bag and then, without melting, 50 mL was transferred into vial (Falcon™ 50mL Conical Centrifuge Tubes) for BC, coarse mode particles number (mix of soil, mineral coarse mode and possibly coal coarse mode) concentration and electrical conductivity analyses. The 85-days experiment was designed with the aim to investigate the BC presence in the upper snow layer, where most of the snow-radiation interaction takes place and where BC particles' presence can decrease the snow albedo (Doherty et al., 2010). Snow albedos increased rapidly and asymptotically as the snow depth increased. Visible albedos reached 0.9 for a snow depth of only 5 cm (Perovich et al. 2007). Moreover, this sampling strategy allowed to evaluate the variation of BC on a seasonal basis and to capture the impacts of wind, precipitation or melting.

During the 3-days experiment, the first 3 cm of surface snow were collected on an hourly basis in pre-cleaned vials in a delimited area of 2 x 2 m using the same sampling tools as above (Spolaor et al., 2019). In this case the samples were collected following a straight line leaving about 5 cm between the sampling points. The aim of the 3-days experiment was to investigate the potential daily cycle of surface BC concentration; therefore, we foresaw that small variations could derive from the impact of the daily variation of short-wave radiation (SWR) and subsequent induced snow metamorphism at the surface of the snowpack, often at cm scale. To avoid dilution of the signal, we reduced the vertical sampling thickness to 3 cm to enhance our chances of observing variation in the rBC mass concentration, if such variation exists.

The temperature at the surface of the snowpack (at 7 cm for 85-days and at 3 cm for 3-days experiment) was always measured. The daily/hourly snow accumulation was determined by measuring the emerging part of 4 poles placed around the sampling area. The average standard deviation calculated from the four poles provides us a reasonable estimate of the variability in snow accumulation\depletion within the sampling area. The standard deviation obtained ranges from 2 to 4 cm for the entire periods, indicating a limited spatial variability.

2.3 Atmospheric Optical Measurements

2.3.1 Aethalometer (AE-31)

In this study, the equivalent BC (eBC) concentration in the Boundary Layer (around 3 m a.s.l) was measured by an AE-31 aethalometer (Gundel et al., 1983), during the 3-day campaign. The device is

equipped with 7-wavelengths (370, 470, 520, 590, 660, 880, 950 nm). It determines the attenuation coefficient by using the light attenuation ratio through a sensing spot and a referenced clean spot, both on a quartz fiber filter substrate. The sampling and reference spots surface areas are 0.5 cm^2, while the volumetric flow rate is 4 L min^{-1}. The flow rate was calibrated with a TetraCal (BGI Instruments) volumetric airflow before and after the field campaign. A 5 minutes temporal resolution was used for data acquisition. However, due to the low background concentration in the Arctic, the signal/noise ratio is high, so that data were hourly averaged. The data presented in this study were processed according to Segura et al. (2014) methodology. For this purpose the multiple scattering and filter loading effect (Weingartner et al., 2003) was corrected with new values of mass absorption cross section (MAC) and multiple scattering factor (C=3.1), reported by Zanatta et al. (2018). The MAC value was derived using observations and observationally constrained Mie calculations in spring at the Zeppelin Arctic station (Svalbard, 78°N). Zanatta et al. (2018) estimated the MAC at 550 nm (9.8 m^2 g^{-1}) and at 880 nm (6.95 m^2 g^{-1}), which we used to estimate MAC at 520 nm (10.2 m^2 g^{-1}).

2.3.2 Particle Soot Absorption Photometer (PSAP)

During the 85-days sampling period the aerosol absorption coefficient was also measured by means of a 3-wavelengths PSAP (this instrument was not available during the 3-days experiment period). It measures the variation of light transmission through a filter where particles are continuously deposited with constant airflow. A second filter identical to the first one remains clean and is used as a reference to take into account possible variations of the light source, i.e. a 3-color LED (blue, green and red with wavelength centred around 470, 530 and 670 nm, respectively). The correction developed by Bond et al. (1999) was applied to consider the filter loading effect. The complete eBC mass concentration time series for the 85-days experiment was retrieved using the Aethalometer (first period) and the PSAP (second period), with an overlapping period with simultaneous measurements of 5 days. For the retrieved eBC mass concentration from the two instruments to be equal during the overlapping period, the PSAP eBC was calculated dividing the absorption measurements (at 530 nm) with a MAC equal to 7.25 m^2 g^{-1} (keeping the AE31 data as reference). Daily averages were calculated from the 1-minute data to compare with the rBC daily data obtained from the snow.

2.4 Surface Snow measurements

2.4.1 Coarse Mode Particles Number Concentration

The snow samples were melted at room temperature before the on-line coarse-mode particles and conductivity measurements (the water was pumped from the vials by a 12 channels peristaltic pump, ISMATECH, type ISM942). Specifically, the number concentration of coarse mode particles in the

surface snow was measured with a Klotz Abakus laser sensor particle counter. This instrument optically counts the total number of particles and measures each particle's size in a liquid constantly flowing through a laser beam cavity (LDS 23/23). The measurements size range of the instrument is from 0.8 to about 80 μm with 32 dimensional bins (Table SI 1), not overlapping with that of the SP2. Only the 32nd bin has a dimensional range above 15.5 μm, i.e. of 80 μm. The data were recorded by a LabView® based software obtaining a sufficient number of data points in order to have a standard deviation less than 5% of the mean value. The particles number concentration was calculated using the constant water flow value.

2.4.2 rBC Measurement – SP2

The rBC mass concentration and mass size distribution were measured following the methods described in Lim et al. (2014). The snow samples were melted at room temperature prior to the analyses. The vials with the melted snow were sonicated for ten minutes at room temperature. The samples were nebulized before the injection in the Apex-Q desolvation system (APEX-Q, Elemental Scientific Inc., Omaha, USA). The nebulization efficiency was evaluated daily by injecting Aquadag® solutions with different mass concentrations, ranging from 0.1 to 100 ng g^{-1}, obtaining an average value of 61%, that was used to correct all the BC mass concentrations reported in this manuscript. More details on the method can be found in Lim et al. (2014) and in Wendl et al. (2014).

The SP2 data were analyzed using the IGOR based toolkit from M. Gysel (Laboratory of Atmospheric Chemistry, Paul Scherrer Institute, Switzerland). The large amount of signals derived from every single particle are elaborated achieving rBC mass and number concentrations and size distributions.

2.5 Meteorological Parameters

Meteorological parameters, in addition to the atmospheric and snow ancillary measurements, were used in the statistical exercise to study the variability of rBC mass concentration in surface snow samples as a function of the atmospheric conditions. BC particles are deposited on the snowpack following a combination of wet and dry deposition. However, once deposited on/in the snowpack other processes can potentially induced a significant variability in the surface BC content. The wind direction and its velocity can modify the BC distribution in the upper snowpack due to snow-mobilization. The solar radiation and relative humidity may enhance snow sublimation and surface hoar formation thus modifying the relative BC concentration in the upper snow layer by removing or adding "water" mass to the snow surface.

Air temperature and relative humidity at 2 meter height have been retrieved from a meteorological station located about 800 meters north of the sampling site, using a ventilated PT-100 thermo-couple by Thies Clima and a HMT337 humicap sensor by Vaisala, respectively. Wind speed and direction at 10 meter

height were obtained from a Combined Wind Sensor Classic by Thies Clima (see Maturilli et al., 2013). At about 50 m distance, the radiation measurements for the Baseline Surface Radiatio Network (BSRN) provide among others the downward solar radiation detected by a Kipp&Zonen CMP22 pyranometer (Maturilli et al., 2015). Both meteorological and surface radiation measurements are available in a 1-minute time resolution via the PANGAEA data repository (Maturilli et al., 2020). The daily/hourly mean values of the meteorological parameters were used in the statistical analyses of the 85-days/3-days experiment and in Figures 2 and 3 (the physical-chemical parameters from the snow samples are punctual values).

2.6 Parameters considered in the statistical analysis

The snowpack evolution is primarily driven by meteorological parameters, which are responsible for adding/removing mass to the annual snowpack. Wind can affect the snow pack evolution in several ways: 1) by snow redistribution, 2) favouring the ablation\sublimation, and 3) lifting particles from nearby sources and areas. Surface snow and air temperatures are two fundamental parameters required to fully understand the varying conditions of the snow pack. In our study, the temperature variables are proxies for the melting episodes and for the presence of liquid water potentially affecting the concentration of impurities. The air and snow temperatures do not have a direct effect in the rBC concertation in surface snow, but they are fundamental indicators to identify the spring warming events ($T > 0°C$, called also the Rain on Snow events - ROS) that yield the snow melting. Moreover, air and snow temperature could be relevant to evaluate possible snow metamorphism and the response of the upper snowpack to the meteorological conditions. Snow and air temperatures can be used during the 3-days experiment to evaluate the daily scale frequency and be helpful to investigate the daily scale variability of rBC in the surface snow.

The SWR is not expected to be directly linked to the surface mass concentration of rBC, however the surface process could affect it indirectly by favouring sublimation (water mass removal), as well as hoar formation (water mass addition) during the colder parts of the day (night/early morning). The relative humidity gives an idea of the amount of water present in the atmosphere and the high RH might favour the deposition of BC suspended by the formation of water droplets through the cloud condensation nuclei. This parameter is especially significant for the selected sampling location, nearby to the shore. Indeed, relative humidity values close or higher than 90% could be associated to fog or low cloud conditions and not directly to wet or dry precipitations. The last meteorological parameter considered is the precipitation amount. This aspect is important to understand the wet deposition processes able to transfer BC particles from the atmosphere to the snow surface.

The additional selected parameters are 1) the atmospheric eBC mass concentration, to investigate the possible link between eBC particles present in the atmosphere and the rBC in snow surface, 2) the coarse mode particles that could have a similar transport pathways to the black carbon and gives an idea of the amount of total impurities deposition and 3) the total water conductivity, an indirect measurement of the salinity content of the snow. It is important to note that the eBC and the rBC mass concentrations are not the same physical quantities: the former is obtained from an absorption measurement assuming a constant MAC, whereas the second is obtained via a laser-induced-incandescence method with an SP2 empirically calibrated with a reference material (Petzold et al., 2013). Considering the location of the sampling site (<1 km from the coastline), the contribution of the ocean emissions to the snowpack chemical composition is significant. We considered the total conductivity as an indication of sea spray deposition, and to investigate common deposition patterns and/or similarities to the behaviour of BC (although BC is not emitted from ocean surface). The conductivity was also considered to determine if there was a large sea-spray aerosol event which could, potentially affecting the SP2 measurements (see supplementary material).

2.7 Statistical Analysis

Multiple linear regression was carried out to evaluate the relationship between the observed surface snow rBC mass concentration and the selected set of covariates consisting of the meteorological and snow physical-chemical parameters that could have a direct effect on controlling snowpack dynamics as well on the BC concentration as discussed in Section 2.6. All the atmospheric parameters described in the previous section (wind, snow and air temperature, incoming solar radiation, relative humidity, and snow precipitation amount) were initially considered as covariates to be included in the multiple linear regression. However, wind speed and direction, as well as the atmospheric stability, expressed as vertical wind speed, were removed because preliminary statistical analyses indicate that none of them is associated with the observed variations in snow rBC mass concentrations. This does not mean that such parameters do not play a role in controlling the BC concentration, but that no statistically significant associations were found with the data collected in our study and thus these parameters were no longer considered in the statistical analyses discussed below.

Multiple linear regression models were fitted on the logarithm scale because the distribution of rBC concentrations in both experiments is characterized by a significant skewness. Coarse mode particles number concentrations and conductivity were also log-transformed to linearize their relationships with log(rBC). The regression model fitted on the two experiments is

$$log(rBC) = \beta_0 + \beta_1\, log(dust) + \beta_2 eBC + \beta_3 temp + \beta_4 snow + \beta_5 swr + \beta_6\, log(cond) + \epsilon.$$

In the above model, 'dust' indicates coarse mode particles number concentrations, 'temp' is the snow temperature at 7 cm depth for the 85-days experiment (daily resolution) and at 2 cm dept for the 3-days experiment (hourly resolution), 'snow' is a binary indicator for the presence of solid precipitation, 'swr' is solar incoming shortwave radiation, 'cond' is the conductivity and ε is a zero-mean normal error. Graphical inspection of residuals plots and normal probability plots confirmed that after the logarithm transformations, the regression models meet the assumptions of linearity, constant error variance (called *homoschedasticity* in the statistical literature) and normal errors. The statistical analyses were performed with the statistical language R (R Core Team, 2020).

3. Results and Discussions

3.1 Seasonal BC variability in surface snow

3.1.1 Atmospheric eBC and atmospheric condition

During the experimental period, the atmospheric eBC concentration ranged between from 80 ng m^{-3} to < 5 ng m^{-3} (Figure 2) with an average of 34 ± 23 ng m^{-3}. The highest concentrations were measured at the beginning of the campaign, especially from April 15th to 27th, followed by a general decreasing trend characterized by the presence of several concentration peaks (on May 8th, 17th and 24th) potentially due to Eurasian fires, as already suggested from Feltracco et al., 2020 (Figure S1). The ammonia daily concentration time series (the only available biomass burning tracer for that period in the area) measured at the Zeppelin station is plotted together with the Gruvebadet atmospheric BC measurements in Figure S3. Biomass burning is a significant source of atmospheric ammonia (Andreae and Merlet, 2001), often affecting the Arctic region (Moroni et al. 2020). As shown in Figure S3, both time series have a similar behaviour at the very beginning of the campaign, from April 3rd to 8th and during the period between May 7th and 21st. This suggests that the BC detected in the atmosphere could be originated from biomass burning episodes during these two time periods. During the 85-days sampling period, wind was characterized by the following median values (25th and 75th percentiles) for direction and speed: 205° (152°, 257°) and 2.7 (1.9, 3.7) m s^{-1}, respectively, therefore mostly coming from south-west (Figure 2). Daily air temperature at 3 m increased during the campaign from -15°C to about +5°C (Figure 2) following the seasonal variation of incoming solar energy: from 100 to 300 W m^{-2} with an average of 185 ± 75 W m^{-2} (Figure 2, orange line). The snow precipitation episodes are presented as daily-accumulated values (Figure 2, blue bars) ranging from zero to 12 cm.

3.1.2 Surface Snow Conditions

Over the 85 days experiment, the snow rBC mass concentration varies from 0.2 to 6 ng g^{-1} (Figure 2), with an average of 1.4 ± 1.3 ng g^{-1}, in agreement with results available in the literature (Mori et al., 2019; Jacobi et al., 2019; Aamaas et al., 2011). An increasing trend can be observed for the rBC mass concentration in the surface snow across the sampling period. The median of the rBC mass equivalent diameter in the snow is 313 ± 35 nm (Figure 2), similar to what obtained in other studies (e.g. Schwarz et al., 2013). The rBC mass equivalent diameter show high variability, ranging from 200 to 500 nm. However, since the rBC concentrations were low, the evaluation of the geometric mean of the particles diameter for the biggest sizes, above 300 to 400 nm, has been considered as qualitative information due to the high signal noise.

The number of coarse mode particles (Figure 2, blue line) shows a constant concentration in the first half of the campaign (1st April - May 11th - average concentration of 3435±1824 # ml^{-1}) whereas it increases in the second half (12th of May to 27th of June - average concentration of 7782±5683 # ml^{-1}), especially after the 1st of June (1st of June to 27th of June - average concentration of 9352±6741 # ml^{-1}), in concomitance with the onset of the snow melting period. The conductivity (Figure 2, green line) also shows an increasing trend at the end of the sampling campaign when snow is melting, with an overall average value of 30 ± 8 μS. The spatial variability of rBC, calculated in the same manner as proposed by Spolaor et al. (2019) for other species, was obtained from six surface snow samples collected in the four corners of the sampling area and two surface snow samples in the centre right before the beginning of the experiment. The following rBC mass concentrations were obtained: a) 3.95 ng g^{-1}; b) 4.92 ng g^{-1} c) 4.20 ng g^{-1}d) 3.10 ng g^{-1}e) 3.82 ng g-1 f) 3.58 ngg^{-1}, resulting in a rBC spatial variability of 16% in the surface snow of the considered sampling area.

3.1.3 Statistical Results

The fitted multiple linear regression model for the 85-days experiment data explains the 69% of the variance of the logarithm of the snow rBC mass concentration ($R^2 = 0.69$). The fitted model indicates the presence of strongly statistically significant associations of the (log transformed) snow rBC mass concentration with the coarse-mode particles number concentration ($p < 0.001$) and the snow temperature ($p < 0.001$). A weaker association is found with the occurrence of snow precipitations ($p = 0.03$). The statistical associations of rBC mass concentration with the other covariates considered in the model are non-significant. See Table 1 for the estimated coefficients and the corresponding p-values.

In order to interpret the statistical results, the description of the 85-days campaign is split into two periods identified as the transition from the “cold” to the “melting” state. The first period occurred before the end of May: the rBC mass concentration often increases with snowfall episodes (April 9th/10th/11th and 17th;

May 17th, 22nd and 27th/28th; June 1st) as suggested by previous studies, with exceptions for April 24th and May 7th. Over the sampling period, a weakly statistically significant positive association ($p = 0.03$) was found between snow rBC mass concentration in surface snow and the occurrence of snow precipitations. BC wet deposition processes are estimated to remove 50% - 60% of the total atmospheric BC burden in the Arctic (Liu et al., 2011; Jacobi et al., 2019). In our study, the wet deposition impacts could be partially masked due to the sampling frequency and the wind snow. In Kongsfjord, a strong wind is often present during the precipitation events (Figure 2). Consequently, the freshly deposited snow is frequently removed from the surface before being able to sample it. Interestingly, our observations show that, on a daily scale, the precipitation episodes are not clearly related to a decrease in the atmospheric eBC mass concentration (Figure 2). A possible explanation is that the precipitation amounts were small so that the precipitation events did not significantly alter the atmospheric BC reservoir.

In the second period, from the beginning of June, the atmospheric temperature increases, causing the snow-melting season's onset. At the beginning of June, the snow rBC mass concentration increases up to approximately 5 ng g^{-1}, and a simultaneous increase was detected in the coarse mode particles number concentration (peaks between June 4th and 7th). As suggested in previous studies, the surface melting process could explain the observed increase in rBC and coarse mode particles concentrations. However, we also have to consider that rBC can be dry deposited, as it has been recently suggested (up to 50-60%; Liu et al., 2011; Jacobi et al., 2019). Very few field validation data exist for estimating the amount of dry deposition at the snow surface, and this process is often used as an ancillary information since most models underestimate the BC in the Arctic snowpack compared to field measurements.

Our data support the hypothesis related to local sources' activation in enhancing the dry deposition impacts in an old mining town as Ny-Alesund. Especially during poor snow cover conditions, as during the snow-melting season, coarse mode particles as residuals of carbon extraction mining activities are available for wind lift\suspension (Vecchiato et al. 2018). The possible effect of local sources' activation is further supported by a recent analysis of the Brøggerbreen glacier and Ny-Ålesund annual snowpack. This analysis shows the presence of retene (an organic compound frequently used to track the presence of coal), most likely due to local sources (Vecchiato et al., 2018).

The simultaneous increase of rBC mass and coarse mode particle number concentrations during the second part of the experiment (e.g. visible between June 3rd and June 7th-8th) could be explained via similar post-depositional processes: snow melting and sublimation. The episodes of snow surface melting can significantly affect the snow particulate content and we hypothesize that the hydrophobicity of pure BC particles, and of several species in the coarse mode particles, might affect its physical location in the

snowpack (in the literature, the response of the BC particles is still debated): the hydrophobicity of the particles can cause the surface concentration to increase while losing water mass through percolation. This could lead into a positive feedback process: the increase of BC concentration can thus enhance snow sublimation (water evaporation) resulting in a further increase of BC concentration in surface snow, and so on.

In this study, the estimated statistical association between snow rBC mass concentration and the daily snow temperature is negative and strongly significant ($p < 0.001$). During the 85-days experiment, we can distinguish two events where the temperature appeared to play a role in the BC concentration. Both of them show an increase in rBC mass concentration during melting/refreezing episodes, in agreement with other studies (Aamaas et al., 2011; Xu et al., 2006; Doherty et al., 2013; Doherty et al. 2016). The first event occurred between May 5th to May 12th and the second event after May 20th, when the proper snow melting began (Figure 2). The first event was characterized by a rapid rise of the daily air temperature (from -6°C to -1°C) in concomitance to a snow precipitation event, followed by a rapid temperature decrease to -6 °C. The surface snow (10 cm) mirrored this behaviour, first rising from -6 °C to 0 °C, and then cooling down to -6 °C. During this warm event, the upper snow strata underwent a melting episode with surface water percolation (although limited), making the surface BC concentration to increase. The second event started approximately on May 20th and lasted until the end of the experiment (Figure 2). During this period, the atmospheric temperature increased constantly, and the snowpack started to melt consequently. Moreover, surface BC concentration increased almost continuously from May 25th to its maximum observed on June 6th. Afterward, the upper snow rBC mass concentration tended to decrease following the rapid snowpack decline.

3.2 Diurnal variation of rBC in surface snow

3.2.1 Surface Snow/Atmospheric Aerosol Content and Atmospheric Conditions

The 3-days experiment was performed at the end of April 2015, during the Arctic spring. The samples were collected on an hourly basis over 3 days achieving a high-resolution sampling frequency. The atmospheric concentration of eBC ranged from 2 to 50 ng m^{-3}, decreasing during the sampling period and not showing any particular diurnal pattern (Figure 3). The mean value of the atmospheric eBC mass concentration is 34 ± 23 ng m^{-3}, similar to the average of the 85-days experiment.

The surface snow rBC mass concentration undergoes to daily time scale change of surface concentration showing up to 2-fold hourly increases (Figure 3, bottom panel, smoothed dark blue line). rBC mass concentrations of approximately 15 ng g^{-1} were measured in the snow samples from the beginning of the sampling to the end of the second day. Later, from the beginning of the third day until

the end of experiment, rBC mass concentrations show an average concentration of about 5 ng g^{-1} (Figure 3). The average value over the whole sampling period is 9 ± 5 ng g^{-1} (approximately 6 times higher than during the 85-days experiment). The rBC mass size distribution was characterized by a median value of the geometric means of about 230 ± 32 nm, significantly lower than that which was measured during the 85-days, and still in agreement with previous studies (Sinha et al., 2018; Schwarz et al., 2013). The concentrations of EC and OC measured in parallel snow samples (not of the same volume) are reported and described in Figure S4; the interpretation of the differences between the rBC and the EC measurements in snow samples was beyond this manuscript's objectives.

The number concentration of coarse mode particles remains stable in the first half of the experiment, until the end of April, and shows an average value over the three days of 26642 ± 9261 # mL^{-3}. The water conductivity shows a similar behaviour, and it is characterized by an average of 39 ± 9 µS (30% higher than during the 85-days experiment).

All the measured snow impurities show two common features (see supplementary material and Figure S4): first, a decrease in the absolute values detected between 4 and 8 a.m. of April 30th, despite the absence of precipitations or any other particular meteorological episode (Figure 3); second, the impact of the snow precipitation event from approximately 4 p.m. to midnight of the April 30th, where the concentrations of aerosols in the snow slightly increased at the very beginning whereas decreasing at the end of the event. Only the BC core diameter remained above the average when the other aerosol snow content decreased (up to approximately 400 nm of mass equivalent diameter), consequently returning to the average value. The spatial variability of BC, calculated as proposed by Spolaor et al. (2019) for other species, was obtained by the analysis of 5 surface snow samples, collected in the four corners of the sampling area and one in the centre obtaining the following concentrations: a) 10.17 ngg^{-1}, b) 10.64 ng g^{-1}, c) 7.04 ngg^{-1}, d) 11.98 ng g^{-1}, and e) 11.91 ng g^{-1}, thus resulting in a spatial variability of 19%. Clear sky conditions where observed for the duration of the sampling period except for the snowfall occurred at the end of the third day.

3.2.2 Statistical Results

The multiple linear regression model for the 3-days experiment explains the 78% of the snow rBC mass concentration variance, a percentage higher than the 85-days experiment, likely due to the more stable atmospheric conditions and the greater interaction with the atmosphere of the upper 3 cm of the snow pack compared with the depth resolution used during the seasonal experiment. Similar for the 85-days experiment we evaluate (Figure S4) the 10 days back-trajectory during the 3 days of the experiment. The result suggests that the air mass arriving in Ny-Ålesund during the experiment were mainly originated from the Arctic Ocean.

The fitted multiple linear regression model indicates a statistically significant association between the logarithm of the rBC mass concentration in the snow and the logarithm of the conductivity ($p < 0.001$), the logarithm of the number concentration of coarse-mode particles ($p < 0.001$) and the occurrence of snow precipitations ($p < 0.001$). The estimated coefficients of the covariates are reported in Table 1. In Figure 4 are displayed the 95% and 90% confidence intervals for the estimated coefficients of regression models fitted to two experiments (85-days and the 3-days). Since the covariates considered in the two experiments have quite different unit scales, Figure 4 shows the confidence intervals for the standardized covariates. The standardization simplifies the comparison among the estimated effects of the different covariates and between the two experiments, in this way allowing a visual comparison of the estimated statistical associations between the logarithm of the snow rBC mass concentration and the considered parameters.

The association between the logarithm of the coarse-mode particles number concentration and the logarithm of the snow rBC mass concentration is positive and strongly significant ($p < 0.001$), similarly to what observed for the 85-days experiment, confirming the similar behaviour of these types of particles also in the surface snow pack (3 cm). The association between the logarithm of conductivity and the logarithm of the snow rBC mass concentration is positive and strongly significant ($p < 0.001$). Snow conductivity is mostly influenced by the presence of sea salt ions (mainly coming from sea spray aerosol considering the location of the experimental site) in the snow samples. Sea spray aerosol is not considered a source of rBC and a direct effect of the sea spray emission on the rBC snow concentration is here consider negligible. However the positive association between rBC and conductivity can be explained by the fact that both sea spray aerosol and BC particles (as well dust) undergoes to similar dry deposition process (when concentration increase) favoured by the stable atmospheric condition occurred during the experiment (with the exception of the snow event during the third day) as well from similar physical removal process (concentration decrease) from the snow surface. Considering we are exploring the rBC concentration change in the upper 3 cm, we explore the possible existence of a daily cycle. The BC particles are known to be non-volatile and not photo-chemically active, therefore the decrease\increase in their concentration observed during the experiment can only be driven by physical process such as wind erosion and snow deposition. However and additional process that might drive the rBC concentration change in the upper snow pack is the condensation of water vapour on the top of the snow crystals and the formation of surface hoar as well the sublimation. The formation of surface hoar has the effect to adding "water" mass without BC particles in the snow surface causing a relative rBC dilution, while sublimation has the effect remove "water" mass causing a relative concentration increase. Surface hoar and sublimation are depending mainly by the temperature and solar radiation, two parameters that exhibits the diurnal cycle (Figure 4). From the statistical analysis no associations were found on rBC with the

incoming solar radiation (at hour resolution) and the snow temperature during the sampling period. These results indicate that the rBC mass concentration in the surface snow does not undergo to diurnal changes and this process are negligible in controlling the rBC snow surface concentration.

The occurrence of snow precipitations is negatively associated with the logarithm of the rBC mass concentration in the snow ($p < 0.001$). As previously remarked, the aerosol scavenging intensity is not measurable with snow sampling strategies based on the sampling of a constant snow thickness from the surface (3 cm in this case). We tentatively explain the negative relation observed in this study with the high frequency sampling, being able to follow the evolution of the BC particles scavenged during a snow episode (from 3 to 12 p.m. of the 30th April 2015). The beginning of the precipitation episodes appeared to remove the highest amount of BC particles, leaving the atmosphere cleaner as reflected by the lower BC mass concentration revealed in subsequent samples. The snow collected at 18:00 of April 30 showed a higher amount of rBC as well as the highest coarse mode particles number concentration and conductivity. In the next few hours, from 9 to 12 p.m., the snow precipitations were depleted in terms of aerosol content and rBC mass concentration.

4. Conclusions and Future Perspectives

The seasonal and daily experiments (85- and 3-days long, respectively) suggest that the rBC concentration in the upper snow layer is not only driven by a cumulative process, as it happens when the entire annual snow pack is evaluated, but it is a rather more complex process involving atmospheric, meteorological and snowpack conditions. Our results based on a multiple linear regression models suggest that the amount of BC in the surface snow is not associated to the BC atmospheric load. This finding suggests that, despite the potentially high atmospheric BC concentrations (as in the case of long-range transport of biomass burning plumes), this parameter does not seem to be the primary driver of the variations in the surface snow rBC over the experiment periods. In both experiments, the coarse mode particles are positively associated with the snow BC mass concentration, suggesting that the BC and coarse mode particles deposition undergo similar deposition and, in case, to post-depositional processes in the upper snowpack. Specifically, before the beginning of the melting season, the wet deposition episodes appeared to have major impacts, whereas the activation of common local sources favour the wind suspension from uncovered areas enhancing the intensity of dry deposition processes, might lead to an accelerated snow melting.

Our results also suggest that in order to explain the observed BC mass concentration variability during seasonal and diurnal time ranges other processes than wet and dry depositions should be considered. Surface melting episodes enrich the BC content in the surface layer not because of an enhanced deposition but mainly because of water mass loss. In particular, the snow mass loss is stronger

during the snow-melting season, where an increase in the rBC concentration could significantly alter the snow albedo and further enhance the radiative absorption, hence promoting a positive feedback. The proposed processes and the rBC concentration determined in Ny-Ålesund could be influenced by local emission in particular at the begging and at the end of the snow season when the snowpack does not cover homogeneously the surface. However, the process described by our results could occur in other Arctic sites although with different magnitudes and impacts.

The remarkable diurnal and daily variability, as well as the complex interdependent mechanisms affecting the rBC mass concentration in the Arctic surface snow, makes the results of albedo-based radiative impact model of the active layer a potential source of erroneous conclusions: the impacts of long distance biomass burning episodes might be overestimated, whereas the impact of local sources and dry deposited impurities during the melting season might be underestimated. Additional empirical studies are therefore necessary in order to improve our understanding of the involved physical mechanisms and to better constrain modelling studies.

Acknowledgements

This work was part of the PhD (in "Science and Management of Climate Change") of Michele Bertò at the Ca' Foscari University of Venice that was partly funded with the Early Human Impact ERC project. Thanks to Giuseppe Pellegrino for helping collecting the samples. Thanks to Jacopo Gabrieli and the technicians of the Ca'Foscari University of Venice for the precious help in building up the coarse mode particles and conductivity measurement apparatus. We acknowledge the use of data and imagery from LANCE FIRMS operated by the NASA/GSFC/Earth Science Data and Information System (ESDIS) with funding provided by NASA/HQ. We want to thank Paolo Laj and the LGGE (Grenoble, France) for lending us the SP2 and Marco Zanatta for transferring the SP2 know-how on instrumental functioning and data analyses. Thanks to Martin Gysel-Beer, PSI, for the IGOR based SP2 Toolkit for SP2 data analyses. We thank Marion Maturilli and AWI for providing us with the meteorological data. Thanks to Giorgio Bertò for checking and correcting the language of this manuscript. This paper is an output of the AMIS project in the framework of "Project MIUR – Dipartimenti di Eccellenza 2018-2022". This project has received funding from the European Union's Horizon 2020 research and innovation programme under grant agreement No 689443 via project iCUPE (Integrative and Comprehensive Understanding on Polar Environments).

Data Availability

Meteorological and surface radiation data are available at the PANGAEA database (Maturilli, 2015a; 2015b; 2015c; 2016a; 2016b; 2018a; 2018b; 2018c; 2018d; 2018e). The data for precipitation amount at Ny-Ålesund can be accessed via the eKlima database of MET Norway. The BC data are available upon request.

Author Contributions

Author contributions. AS, EB, DC and MB conceived the experiments; AS, EB, DC, and LP collected the samples; MB measured the samples; KM and MMaz provided the atmospheric eBC concentrations; SC and DC provided the back-trajectories analyses; CV performed the statistical analyses with inputs from MB and AS. MB prepared the manuscript mainly with inputs from AS, J-C. G and DC (in the methods section from AS, KM, MMaz) and all co-authors contributed to the interpretation of the results as well as manuscript review and editing.

Data repository

Maturilli, Marion (2020): Basic and other measurements of radiation and continuous meteorological observations at station Ny-Ålesund (April, May 2014 and April, May, June 2015), reference list of 10 datasets. Alfred Wegener Institute - Research Unit Potsdam, PANGAEA, https://doi.pangaea.de/10.1594/PANGAEA.913988 (DOI registration in progress)

FIGURES

Figure 1. a) Experimental sampling site location (dark grey rectangle), in proximity of the Gruvebadet Aerosol Laboratory. b) Gruvebadet area (black square), close to the Ny-Ålesund research village. From: Spolaor et al., 2019 (maps from https://toposvalbard.npolar.no/). The red arrow points to the North.

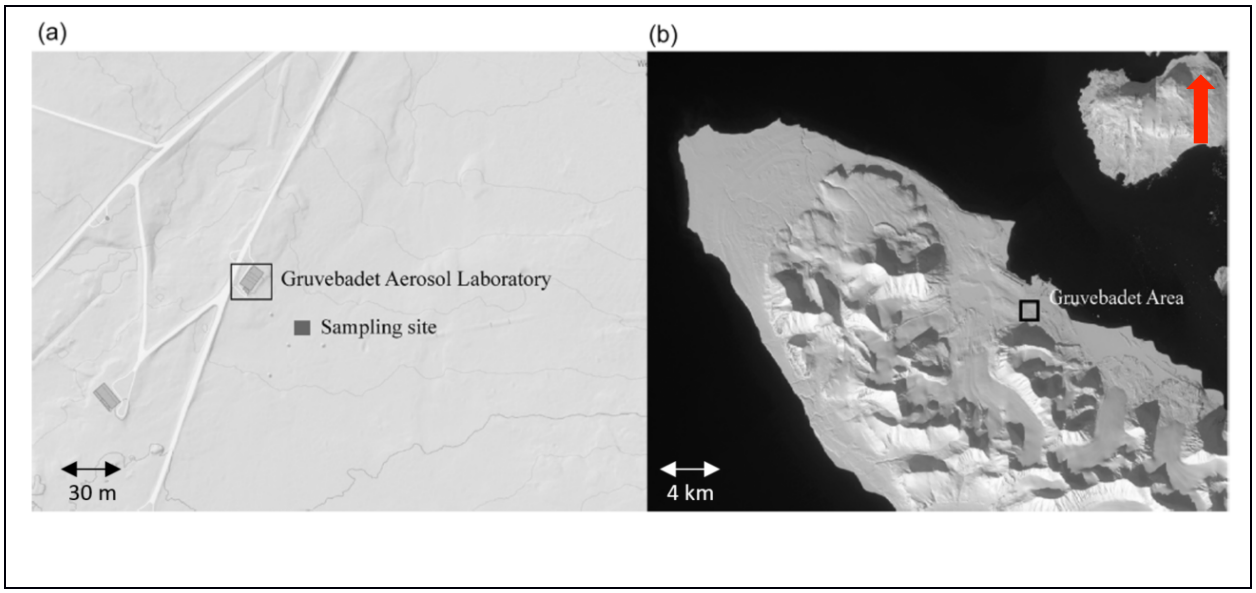

Figure 2. The 85-days experiments daily snow samples rBC mass concentration (light blue), eBC mass concentration in the atmosphere (black), geometric mean mass equivalent diameter (purple), number of coarse mode particles (Cmp - blue), total conductivity (green), meteo/snow parameters used in the statistical exercise: wind speed color coded for wind direction, solar radiation (orange line), air and surface snow temperatures (blue bars and green line respectively), amount of fresh snow ("snow precipitations", light blue bars) and the snow accumulation ("Neg. accumulation"; the values where multiplied by -1 in order to show the similar trend of the snow lost and of the air/snow temperature during the melting period at the end of the campaign).

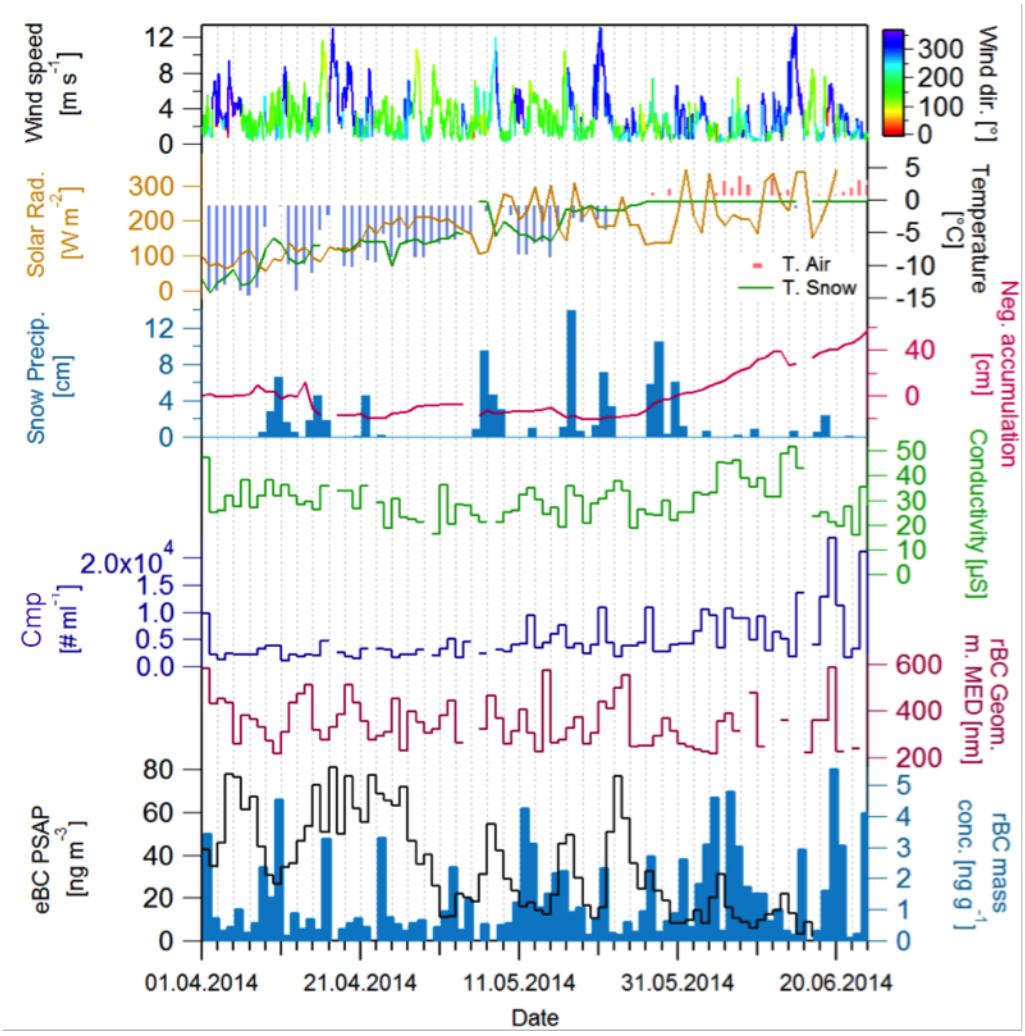

Figure 3. The 3-days experiments snow samples hourly rBC mass concentration and smoothed line (light blue bars), atmospheric eBC mass concentration in the atmosphere (black), geometric mean mass equivalent diameter (purple), the number concentration of coarse mode particles (Cmp - blue) and the total conductivity (green), meteo/snow parameters used in the statistical exercise: wind speed color coded for wind direction, solar radiation (Orange line), Air and surface snow temperature (blue bars and green line respectively), amount of fresh snow ("snow precipitations", light blue bars). The yellow bars are centered on the midnight hours for the three sampling days.

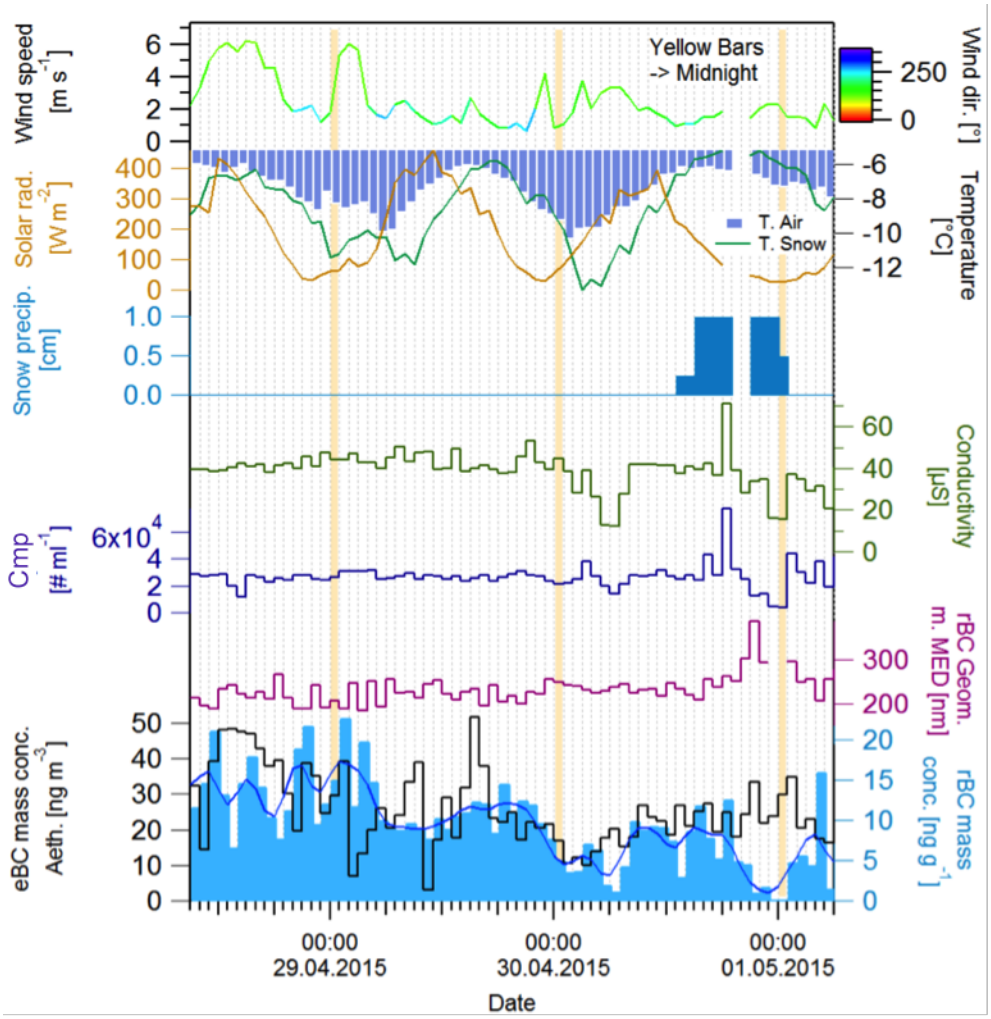

Figure 4. Estimated coefficients of the standardized covariates of the multiple linear regression models fitted to the 3 days and 85 days experiments. The segments correspond to 95% confidence intervals about the corresponding estimated coefficients. The internal thicker segments correspond to 90% confidence intervals. Intervals, that do not include the zero, correspond to statistically significant covariates. If a confidence interval consists of positive values, then there is a significant positive association between the corresponding covariate and the logarithm of the snow rBC mass concentration given the remaining covariates. Vice versa, if the confidence interval consists of negative values, then the association is negative. The abbreviations used in the plot are: "log(cond)" – logarithm of the water conductivity time series, "log(dust)" – logarithm of the coarse mode particles number concentration time series, "eBC" – equivalent black carbon atmospheric concentration, "snow" – presence of snow precipitation episodes, "swr" – short wave radiation, "temp" – the snow temperature. The plot is produced with the R package (R Core Team, 2020) jtools (Long, 2020).

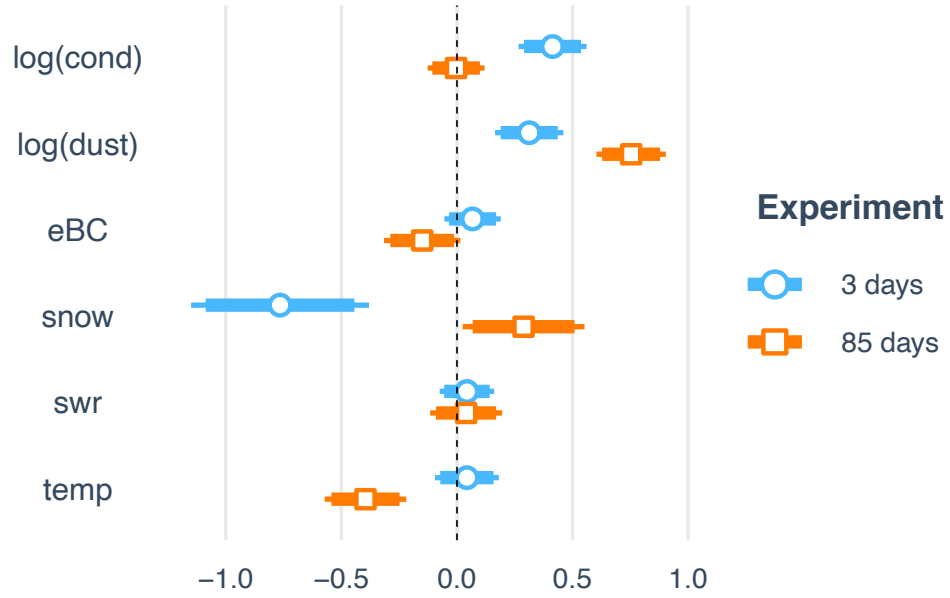

TABLES

Table 1. Estimated coefficients, 95% confidence intervals and the corresponding p-values for the covariates of the multiple linear regression model fitted to the 85 days and the 3-days experiments. The last rows of the table report the number of observations, the multiple coefficient of determination (R^2) and its adjusted version.

	85-days			**3-days**		
Covariates	*Estimates*	*CI*	*p*	*Estimates*	*CI*	*p*
(Intercept)	-6.74	-8.74 – -4.74	**<0.001**	1.39	-2.30 – 5.09	0.453
Cond[log]	-0.02	-0.51 – 0.48	0.950	1.38	0.89 – 1.87	**<0.001**
Dust[log]	1.29	1.03 – 1.55	**<0.001**	0.74	0.39 – 1.09	**<0.001**
eBC	-0.01	-0.01 – 0.00	0.074	0.00	-0.00 – 0.01	0.272
Snow[TRUE]	0.29	0.02 – 0.55	**0.033**	-0.77	-1.15 – -0.38	**<0.001**
SWR	0.00	-0.00 – 0.00	0.613	0.00	-0.00 – 0.00	0.468
Temp	-0.10	-0.14 – -0.05	**<0.001**	0.02	-0.04 – 0.08	0.535
Observation	72			68		
R2 /R2 adjusted	0.688/0.6590			0.779 /0.758		

References

Aamaas, B., Bøggild, C. E., Stordal, F., Berntsen, T., Holmèn, K. and Strùm, J.: Elemental carbon deposition to Svalbard snow from Norwegian settlements and long-range transport, Tellus B Chem. Phys. Meteorol., 63(3), 340–351, doi:10.1111/j.1600-0889.2011.00531.x, 2011.

AMAP, A. M. and A.: ARCTIC MONITORING AND ASSESSMENT PROGRAMME (AMAP): Work Plan 2015–2017., Working Paper, Arctic Monitoring and Assessment Programme (AMAP). [online] Available from: https://oaarchive.arctic-council.org/handle/11374/1443 (Accessed 6 May 2020), 2015.

Andreae, M. O. and Merlet, P.: Emission of trace gases and aerosols from biomass burning, Glob. Biogeochem. Cycles, 15(4), 955–966, doi:10.1029/2000GB001382, 2001.

Bazzano, A., Ardini, F., Becagli, S., Traversi, R., Udisti, R., Cappelletti, D. and Grotti, M.: Source assessment of atmospheric lead measured at Ny-Ålesund, Svalbard, Atmos. Environ., 113, 20–26, doi:10.1016/j.atmosenv.2015.04.053, 2015.

Bond, T. C., Anderson, T. L. and Campbell, D.: Calibration and Intercomparison of Filter-Based Measurements of Visible Light Absorption by Aerosols, Aerosol Sci. Technol., 30(6), 582–600, doi:10.1080/027868299304435, 1999.

Bond, T. C., Doherty, S. J., Fahey, D. W., Forster, P. M., Berntsen, T., DeAngelo, B. J., Flanner, M. G., Ghan, S., Kärcher, B., Koch, D., Kinne, S., Kondo, Y., Quinn, P. K., Sarofim, M. C., Schultz, M. G., Schulz, M., Venkataraman, C., Zhang, H., Zhang, S., Bellouin, N., Guttikunda, S. K., Hopke, P. K., Jacobson, M. Z., Kaiser, J. W., Klimont, Z., Lohmann, U., Schwarz, J. P., Shindell, D., Storelvmo, T., Warren, S. G. and Zender, C. S.: Bounding the role of black carbon in the climate system: A scientific assessment: BLACK CARBON IN THE CLIMATE SYSTEM, J. Geophys. Res. Atmospheres, 118(11), 5380–5552, doi:10.1002/jgrd.50171, 2013.

Cohen, J., Screen, J. A., Furtado, J. C., Barlow, M., Whittleston, D., Coumou, D., Francis, J., Dethloff, K., Entekhabi, D., Overland, J. and Jones, J.: Recent Arctic amplification and extreme mid-latitude weather, Nat. Geosci., 7(9), 627–637, doi:10.1038/ngeo2234, 2014.

Comiso, J. C., Parkinson, C. L., Gersten, R. and Stock, L.: Accelerated decline in the Arctic sea ice cover, Geophys. Res. Lett., 35(1), doi:10.1029/2007GL031972, 2008.

DeMott, P.J., Hill, T.C., McCluskey, C.S., Prather, K.A., Collins, D.B., Sullivan, R.C., Ruppel, M.J., Mason, R.H., Irish, V.E., Lee, T. and Hwang, C.Y.: Sea spray aerosol as a unique source of ice nucleating particles. Proceedings of the National Academy of Sciences, 113(21), pp.5797-5803, doi: 10.1073/pnas.1514034112, 2016.

Doherty, S. J., S. G. Warren, T. C. Grenfell, A. D. Clarke, and R. E. Brandt.: Light-absorbing impurities in Arctic snow. Atmospheric Chem. Phys.10, no. 23: 11647, doi: 10.5194/acp-10-11647-2010, 2010.

Doherty, S. J., T. C. Grenfell, S. Forsström, D. L. Hegg, S. G. Warren and R. Brandt, Observed vertical redistribution of black carbon and other light-absorbing particles in melting snow, J. Geophys. Res., 118(11), 5553-5569, doi:10.1002/jgrd.50235, 2013.

Doherty, S. J., D. A. Hegg, P. K. Quinn, J. E. Johnson, J. P. Schwarz, C. Dang and S. G. Warren, Causes of variability in light absorption by particles in snow at sites in Idaho and Utah, J. Geophys. Res. - Atmos., 121, doi:10.1002/2015JD024375, 2016.

706 Eckhardt, S., Hermansen, O., Grythe, H., Fiebig, M., Stebel, K., Cassiani, M., Baecklund, A. and Stohl,
707 A.: The influence of cruise ship emissions on air pollution in Svalbard - a harbinger of a more polluted
708 Arctic?, Atmospheric Chem. Phys., 13(16), 8401–8409, doi: 10.5194/acp-13-8401-2013, 2013.

709 Eckhardt, S., Quennehen, B., Oliviè, D. J. L., Berntsen, T. K., Cherian, R., Christensen, J. H., W. Collins
710 et al.:Current model capabilities for simulating black carbon and sulfate concentrations in the Arctic
711 atmosphere: a multi-model evaluation using a comprehensive measurement data set. Atmospheric
712 Chem. Phys., 15, no. 16: 9413-9433, doi: 10.5194/acp-15-9413-2015, 2015.

713 Eleftheriadis, K., Vratolis, S. and Nyeki, S.: Aerosol black carbon in the European Arctic: Measurements
714 at Zeppelin station, Ny-Ålesund, Svalbard from 1998–2007, Geophys. Res. Lett., 36(2),
715 doi:10.1029/2008GL035741, 2009.

716 Feltracco, M., Barbaro, E., Kirchgeorg, T., Spolaor, A., Turetta, C., Zangrando, R., Barbante, C. and
717 Gambaro, A.: Free and combined L- and D-amino acids in Arctic aerosol, Chemosphere, 220, 412–421,
718 doi:10.1016/j.chemosphere.2018.12.147, 2019.

719 Feltracco, M., Barbaro, E., Tedeschi, S., Spolaor, A., Turetta, C., Vecchiato, M., Morabito, E.,
720 Zangrando, R., Barbante, C. and Gambaro, A.: Interannual variability of sugars in Arctic aerosol:
721 Biomass burning and biogenic inputs, Sci. Total Environ., 706, 136089,
722 doi:10.1016/j.scitotenv.2019.136089, 2020.

723 Feltracco, M., Barbaro, E., Spolaor, A., Vecchiato, M., Callegaro, A., Burgay, F., Vardè, M., Maffezzoli,
724 N., Dallo, F., Scoto, F., Zangrando, R., Barbante, C., Gambaro, A.: Year-round measurements of size-
725 segregated low molecular weight organic acids in Arctic aerosol. Sci. Total Environ., 763, 142954, doi:
726 10.1016/j.scitotenv.2020.142954, 2021a.

727 Feltracco, M., Barbaro, E., Hoppe, C. J., Wolf, K. K., Spolaor, A., Layton, R., Keuschnig, C., Barbante,
728 C., Gambaro, A., Larose, C.: Airborne bacteria and particulate chemistry capture Phytoplankton bloom
729 dynamics in an Arctic fjord, Atmos. Environ., 256, 118458, doi: 10.1016/j.atmosenv.2021.118458,
730 2021b.

731 Ferrero, L., Cappelletti, D., Busetto, M., Mazzola, M., Lupi, A., Lanconelli, C., Becagli, S., Traversi, R.,
732 Caiazzo, L., Giardi, F., Moroni, B., Crocchianti, S., Fierz, M., Mocnik, G., Sangiorgi, G., Perrone, M.
733 G., Maturilli, M., Vitale, V., Udisti, R. and Bolzacchini, E.: Vertical profiles of aerosol and black carbon
734 in the Arctic: a seasonal phenomenology along two years (2011-2012) of field campaign, Atmospheric
735 Chem. Phys., 16, 12601–12629, doi: 10.5194/acp-16-12601-2016, hdl:10013/epic.48736, 2016.

736 Flanner, M. G.: Arctic climate sensitivity to local black carbon, J. Geophys. Res. Atmospheres, 118(4),
737 1840–1851, doi:10.1002/jgrd.50176, 2013.

738 Flanner, M. G., Zender, C. S., Randerson, J. T. and Rasch, P. J.: Present-day climate forcing and response
739 from black carbon in snow, J. Geophys. Res. Atmospheres, 112(D11), doi:10.1029/2006JD008003,
740 2007.

741 Forsström, S., Ström, J., Pedersen, C. A., Isaksson, E. and Gerland, S.: Elemental carbon distribution in
742 Svalbard snow, J. Geophys. Res. Atmospheres, 114(D19), doi:10.1029/2008JD011480, 2009.

743 Forsström, S., Isaksson, E., Skeie, R. B., Ström, J., Pedersen, C. A., Hudson, S. R., Berntsen, T. K.,
744 Lihavainen, H., Godtliebsen, F. and Gerland, S.: Elemental carbon measurements in European Arctic
745 snowpacks, J. Geophys. Res. Atmospheres, 118(24), 13,614-13,627, doi:10.1002/2013JD019886, 2013.

Gallet JC, Björkman M, Larose C, Luks B., Martma T. and Zdanowics C. (eds). Protocols and recommendations for the measurement of snow physical properties, and sampling of snow for black carbon, water isotopes, major ions and micro-organisms. Norwegian Polar Institute. Kortrapport / Brief Report no. 046, ISBN 978-82-7666-415-7 (printed), www.npolar.no, 2018.

Gogoi, M. M., Babu, S. S., Moorthy, K. K., Thakur, R. C., Chaubey, J. P. and Nair, V. S.: Aerosol black carbon over Svalbard regions of Arctic, Polar Sci., 10(1), 60–70, doi:10.1016/j.polar.2015.11.001, 2016.

Gundel, L. A., Dod, R. L., Rosen, H. and Novakov, T.: Relationship between optical attenuation and black carbon concentration for ambient and source particles, Lawrence Berkeley Lab., CA (USA). [online] Available from: https://www.osti.gov/biblio/5653266 (Accessed 7 May 2020), 1983.

Hadley, O. L. and Kirchstetter, T. W.: Black-carbon reduction of snow albedo, Nat. Clim. Change, 2(6), 437–440, doi:10.1038/nclimate1433, 2012.

Hansen, J. and Nazarenko, L.: Soot climate forcing via snow and ice albedos, Proc. Natl. Acad. Sci., 101(2), 423–428, doi:10.1073/pnas.2237157100, 2004.

Ingersoll, G.P., Don Campbell, M. Alisa Mast, David W. Clow, Leora Nanus, and Brent Frakes. 2009. Snowpack Chemistry Monitoring Protocol for the Rocky Mountain Network; Narrative and Standard Operating Procedures. United States Geological Service (USGS), Reston, Virginia. Administrative Report, 2009

Jacobi, H.-W., Obleitner, F., Da Costa, S., Ginot, P., Eleftheriadis, K., Aas, W. and Zanatta, M.: Deposition of ionic species and black carbon to the Arctic snowpack: combining snow pit observations with modeling, 10361-10377, doi:10.5194/acp-19-10361-2019, 2019.

Khan, A. L., Dierssen, H., Schwarz, J. P., Schmitt, C., Chlus, A., Hermanson, M., Painter, T. H. and McKnight, D. M.: Impacts of coal coarse mode from an active mine on the spectral reflectance of Arctic surface snow in Svalbard, Norway, J. Geophys. Res. Atmospheres, 122(3), 1767–1778, doi:10.1002/2016JD025757, 2017.

Laborde, M., Crippa, M., Tritscher, T., Jurányi, Z., Decarlo, P. F., Temime-Roussel, B., Marchand, N., Eckhardt, S., Stohl, A., Baltensperger, U., Prévôt, A. S. H., Weingartner, E. and Gysel, M.: Black carbon physical properties and mixing state in the European megacity Paris, Atmospheric Chem. Phys., 13(11), 5831–5856, doi:10.5194/acp-13-5831-2013, 2013.

Laj, P., Bigi, A., Rose, C., Andrews, E., Lund Myhre, C., Collaud Coen, M., Wiedensohler, A., Schultz, M., Ogren, J. A., Fiebig, M., Gliß, J., Mortier, A., Pandolfi, M., Petäjä, T., Kim, S.-W., Aas, W., Putaud, J.-P., Mayol-Bracero, O., Keywood, M., Labrador, L., Aalto, P., Ahlberg, E., Alados Arboledas, L., Alastuey, A., Andrade, M., Artíñano, B., Ausmeel, S., Arsov, T., Asmi, E., Backman, J., Baltensperger, U., Bastian, S., Bath, O., Beukes, J. P., Brem, B. T., Bukowiecki, N., Conil, S., Couret, C., Day, D., Dayantolis, W., Degorska, A., Santos, S. M. D., Eleftheriadis, K., Fetfatzis, P., Favez, O., Flentje, H., Gini, M. I., Gregorič, A., Gysel-Beer, M., Hallar, G. A., Hand, J., Hoffer, A., Hueglin, C., Hooda, R. K., Hyvärinen, A., Kalapov, I., Kalivitis, N., Kasper-Giebl, A., Kim, J. E., Kouvarakis, G., Kranjc, I., Krejci, R., Kulmala, M., Labuschagne, C., Lee, H.-J., Lihavainen, H., Lin, N.-H., Löschau, G., Luoma, K., Marinoni, A., Meinhardt, F., Merkel, M., Metzger, J.-M., Mihalopoulos, N., Nguyen, N. A., Ondracek, J., Peréz, N., Perrone, M. R., Petit, J.-E., Picard, D., Pichon, J.-M., Pont, V., Prats, N., Prenni, A., Reisen, F., Romano, S., Sellegri, K., Sharma, S., Schauer, G., Sheridan, P., Sherman, J. P., Schütze, M., Schwerin, A., Sohmer, R., Sorribas, M., Steinbacher, M., Sun, J., Titos, G., Tokzko, B., et al.: A

global analysis of climate-relevant aerosol properties retrieved from the network of GAW near-surface observatories, Atmospheric Meas. Tech. Discuss., 1–70, doi: 10.5194/amt-2019-499, 2020.

Law, K. S. and Stohl, A.: Arctic Air Pollution: Origins and Impacts, Science, 315(5818), 1537–1540, doi:10.1126/science.1137695, 2007.

Lim, S., Fain, X., Zanatta, M., Cozic, J., Jaffrezo, J. L., Ginot, P. and Laj, P.: Refractory black carbon mass concentrations in snow and ice: method evaluation and inter-comparison with elemental carbon measurement, Atmospheric Meas. Tech., 7(10), 3307–3324, doi:10.5194/amt-7-3307-2014, 2014.

Liu, J., Fan, S., Horowitz, L. W. and Levy, H.: Evaluation of factors controlling long-range transport of black carbon to the Arctic, J. Geophys. Res. Atmospheres, 116(D4), doi:10.1029/2010JD015145, 2011.

Long J.A.. jtools: Analysis and Presentation of Social Scientific Data (2020). URL: https://cran.r-project.org/package=jtools

Lupi, A., Busetto, M., Becagli, S., Giardi, F., Lanconelli, C., Mazzola, M., Udisti, R., Hansson, H.-C., Henning, T., Petkov, B., Ström, J., Krejci, R., Tunved, P., Viola, A. P. and Vitale, V.: Multi-seasonal ultrafine aerosol particle number concentration measurements at the Gruvebadet observatory, Ny-Ålesund, Svalbard Islands, Rendiconti Lincei, 27(1), 59–71, doi:10.1007/s12210-016-0532-8, 2016.

Maturilli, M., Herber, A. and König-Langlo, G.: Climatology and Time Series of Surface Meteorology in Ny¬Ålesund, Svalbard, Earth Syst. Sci. Data, 5, 155–163, doi: 10.5194/essd-5-155-2013, 2013.

Maturilli, M., Herber, A. and König-Langlo, G.: Surface radiation climatology for Ny-Ålesund, Svalbard (78.9° N), basic observations for trend detection, Theor. Appl. Climatol., 120(1), 331–339, doi:10.1007/s00704-014-1173-4, 2015.

Maturilli, M., Hanssen-Bauer, I., Neuber, R., Rex, M. and Edvardsen, K.: The Atmosphere Above Ny-Ålesund: Climate and Global Warming, Ozone and Surface UV Radiation, in The Ecosystem of Kongsfjorden, Svalbard, edited by H. Hop and C. Wiencke, pp. 23–46, Springer International Publishing, Cham., 2019.

Meinander, O.; Heikkinen, E.; Aurela, M.; Hyvärinen, A. Sampling, Filtering, and Analysis Protocols to Detect Black Carbon, Organic Carbon, and Total Carbon in Seasonal Surface Snow in an Urban Background and Arctic Finland (>60° N). Atmosphere 2020, 11, 923. https://doi.org/10.3390/atmos11090923, 2020a.

Moosmüller, H., Chakrabarty, R. K. and Arnott, W. P.: Aerosol light absorption and its measurement: A review, J. Quant. Spectrosc. Radiat. Transf., 110(11), 844–878, doi:10.1016/j.jqsrt.2009.02.035, 2009.

Mori, T., Goto‐Azuma, K., Kondo, Y., Ogawa‐Tsukagawa, Y., Miura, K., Hirabayashi, M., Oshima, N., Koike, M., Kupiainen, K., Moteki, N., Ohata, S., Sinha, P. R., Sugiura, K., Aoki, T., Schneebeli, M., Steffen, K., Sato, A., Tsushima, A., Makarov, V., Omiya, S., Sugimoto, A., Takano, S. and Nagatsuka, N.: Black Carbon and Inorganic Aerosols in Arctic Snowpack, J. Geophys. Res. Atmospheres, 124(23), 13325–13356, doi:10.1029/2019JD030623, 2019.

Moroni, B., Becagli, S., Bolzacchini, E., Busetto, M., Cappelletti, D., Crocchianti, S., Ferrero, L., Frosini, D., Lanconelli, C., Lupi, A., Maturilli, M., Mazzola, M., Perrone, M. G., Sangiorgi, G., Traversi, R., Udisti, R., Viola, A. and Vitale, V.: Vertical Profiles and Chemical Properties of Aerosol Particles upon Ny-Ålesund (Svalbard Islands), Adv. Meteorol., 2015, e292081, doi: 10.1155/2015/292081, 2015.

826 Moroni, B., Arnalds, O., Dagsson-Waldhauserová, P., Crocchianti, S., Vivani, R. and Cappelletti, D.:
827 Mineralogical and Chemical Records of Icelandic Coarse mode Sources Upon Ny-Ålesund (Svalbard
828 Islands), Front. Earth Sci., 6, doi:10.3389/feart.2018.00187, 2018.

829 Moroni, B., Ritter, C., Crocchianti, S., Markowicz, K., Mazzola, M., Becagli, S., et al.. Individual particle
830 characteristics, optical properties and evolution of an extreme long‐range transported biomass burning
831 event in the European Arctic (Ny‐Ålesund, Svalbard Islands). Journal of Geophysical Research:
832 Atmospheres, 125, e2019JD031535, doi:10.1029/2019JD031535, 2020.
833

834 Motos, G., Schmale, J., Corbin, J. C., Modini, R. L., Karlen, N., Bertò, M., Baltensperger, U. and Gysel-
835 Beer, M.: Cloud droplet activation properties and scavenged fraction of black carbon in liquid-phase
836 clouds at the high-alpine research station Jungfraujoch (3580 m a.s.l.), Atmospheric Chem. Phys., 19(6),
837 3833–3855, doi:10.5194/acp-19-3833-2019, 2019.

838 Osmont, D., Wendl, I. A., Schmidely, L., Sigl, M., Vega, C. P., Isaksson, E. and Schwikowski, M.: An
839 800-year high-resolution black carbon ice core record from Lomonosovfonna, Svalbard, Atmospheric
840 Chem. Phys., 18(17), 12777–12795, doi: 10.5194/acp-18-12777-2018, 2018.

841 Pedersen, C. A., Gallet, J.-C., Ström, J., Gerland, S., Hudson, S. R., Forsström, S., Isaksson, E. and
842 Berntsen, T. K.: In situ observations of black carbon in snow and the corresponding spectral surface
843 albedo reduction, J. Geophys. Res. Atmospheres, 120(4), 1476–1489, doi: 10.1002/2014JD022407,
844 2015.

845 Perovich, D. : Light reflection and transmission by a temperate snow cover. *Journal of Glaciology,*
846 *53*(181), 201-210. doi:10.3189/172756507782202919, 2007
847

848 Petzold, A., Ogren, J. A., Fiebig, M., Laj, P., Li, S.-M., Baltensperger, U., Holzer-Popp, T., Kinne, S.,
849 Pappalardo, G., Sugimoto, N., Wehrli, C., Wiedensohler, A. and Zhang, X.-Y.: Recommendations for
850 reporting "black carbon" measurements, Atmospheric Chem. Phys., 13(16), 8365–8379, doi:
851 10.5194/acp-13-8365-2013, 2013.

852 R Core Team. R: A language and environment for statistical computing. R Foundation for Statistical
853 Computing, Vienna, Austria, (2020). URL: https://www.R-project.org/

854 Ruppel, M. M., Soares, J., Gallet, J.-C., Isaksson, E., Martma, T., Svensson, J., Kohler, J., Pedersen, C.
855 A., Manninen, S., Korhola, A. and Ström, J.: Do contemporary (1980–2015) emissions determine the
856 elemental carbon deposition trend at Holtedahlfonna glacier, Svalbard?, Atmospheric Chem. Phys.,
857 17(20), 12779–12795, doi: 10.5194/acp-17-12779-2017, 2017.

858 Scalabrin, E., Zangrando, R., Barbaro, E., Kehrwald, N. M., Gabrieli, J., Barbante, C. and Gambaro, A.:
859 Amino acids in Arctic aerosols, Atmospheric Chem. Phys., 12(21), 10453–10463, doi:10.5194/acp-12-
860 10453-2012, 2012.

861 Schmale, J., Arnold, S. R., Law, K. S., Thorp, T., Anenberg, S., Simpson, W. R., Mao, J. and Pratt, K. A.:
862 Local Arctic Air Pollution: A Neglected but Serious Problem, Earths Future, 6(10), 1385–1412,
863 doi:10.1029/2018EF000952, 2018.

864 Schwarz, J. P., Gao, R. S., Perring, A. E., Spackman, J. R. and Fahey, D. W.: Black carbon aerosol size in
865 snow, Sci. Rep., 3(1), 1–5, doi:10.1038/srep01356, 2013.

866 Screen, J. A. and Simmonds, I.: The central role of diminishing sea ice in recent Arctic temperature
867 amplification, Nature, 464(7293), 1334–1337, doi:10.1038/nature09051, 2010.

868 Segura, S., Estellés, V., Titos Vela, G., Lyamani, H., Utrilla Navarro, P., Zotter, P., Prévot, A. S. H.,
869 Močnik, G., Alados-Arboledas, L. and Martínez-Lozano, J. A.: Determination and analysis of in situ
870 spectral aerosol optical properties by a multi-instrumental approach, doi:10.5194/amt-7-2373-2014,
871 2014.

872 Serreze, M. C. and Barry, R. G.: Processes and impacts of Arctic amplification: A research synthesis,
873 Glob. Planet. Change, 77(1), 85–96, doi:10.1016/j.gloplacha.2011.03.004, 2011.

874 Sharma, S., W. Richard Leaitch, Lin Huang, Daniel Veber, Felicia Kolonjari, Wendy Zhang. An
875 evaluation of three methods for measuring black carbon in Alert, Canada. Atmos. Chem. Phys., 17,
876 15225-15243, https://doi.org/10.5194/acp-17-15225-2017, 2017.

877 Sinha, P. R., Y. Kondo, M. Koike, J. Ogren, A. Jefferson, T. Barrett, R. Sheesley, S. Ohata, N. Moteki, H.
878 Coe, D. Liu, M. Irwin, P. Tunved, P. K. Quinn, and Y. Zhao, Evaluation of ground-based black carbon
879 measurements by filter-based photometers at two Arctic sites, J. Geophys. Res., 122,
880 doi:10.1002/2016JJD025843, 2017.

881 Sinha, P. R., Kondo, Y., Goto-Azuma, K., Tsukagawa, Y., Fukuda, K., Koike, M., Ohata, S., Moteki, N.,
882 Mori, T., Oshima, N., Førland, E. J., Irwin, M., Gallet, J.-C. and Pedersen, C. A.: Seasonal Progression
883 of the Deposition of Black Carbon by Snowfall at Ny-Ålesund, Spitsbergen: Deposition of Black
884 Carbon in Spitsbergen, J. Geophys. Res. Atmospheres, 123(2), 997–1016, doi:10.1002/2017JD028027,
885 2018.

886 Skiles, S. M. and Painter, T. H.: Toward Understanding Direct Absorption and Grain Size Feedbacks by
887 Coarse mode Radiative Forcing in Snow With Coupled Snow Physical and Radiative Transfer
888 Modeling, Water Resour. Res., 55(8), 7362–7378, doi:10.1029/2018WR024573, 2019.

889 Skiles, S. M., Flanner, M., Cook, J. M., Dumont, M. and Painter, T. H.: Radiative forcing by light-
890 absorbing particles in snow, Nat. Clim. Change, 8(11), 964–971, doi:10.1038/s41558-018-0296-5, 2018.

891 Spolaor, A., Angot, H., Roman, M., Dommergue, A., Scarchilli, C., Vardè, M., Del Guasta, M., Pedeli,
892 X., Varin, C., Sprovieri, F., Magand, O., Legrand, M., Barbante, C. and Cairns, W. R. L.: Feedback
893 mechanisms between snow and atmospheric mercury: Results and observations from field campaigns on
894 the Antarctic plateau, Chemosphere, 197, 306–317, doi:10.1016/j.chemosphere.2017.12.180, 2018.

895 Spolaor, A., Barbaro, E., Cappelletti, D., Turetta, C., Mazzola, M., Giardi, F., Björkman, M. P.,
896 Lucchetta, F., Dallo, F., Pfaffhuber, K. A., Angot, H., Dommergue, A., Maturilli, M., Saiz-Lopez, A.,
897 Barbante, C. and Cairns, W. R. L.: Diurnal cycle of iodine, bromine, and mercury concentrations in
898 Svalbard surface snow, Atmospheric Chem. Phys., 19(20), 13325–13339, doi: 10.5194/acp-19-13325-
899 2019, 2019.

900 Stephens, M., Turner, N. and Sandberg, J.: Particle identification by laser-induced incandescence in a
901 solid-state laser cavity, Appl. Opt., 42(19), 3726–3736, doi:10.1364/AO.42.003726, 2003.

902 Stohl, A., Klimont, Z., Eckhardt, S., Kupiainen, K., Shevchenko, V. P., Kopeikin, V. M., and Novigatsky,
903 A. N.: Black carbon in the Arctic: the underestimated role of gas flaring and residential combustion
904 emissions., Atmospheric Chem. Phys., 13(17), 8833-8855, doi: 10.5194/acp-13-8833-2013, 2013.

Tunved, P., Ström, J. and Krejci, R.: Arctic aerosol life cycle: linking aerosol size distributions observed between 2000 and 2010 with air mass transport and precipitation at Zeppelin station, Ny-Ålesund, Svalbard, Atmospheric Chem. Phys., 13(7), 3643–3660, doi: 10.5194/acp-13-3643-2013, 2013.

Turetta, C., Feltracco, M., Barbaro, E., Spolaor, A., Barbante, C., & Gambaro, A.: A Year-Round Measurement of Water-Soluble Trace and Rare Earth Elements in Arctic Aerosol: Possible Inorganic Tracers of Specific Events, Atmosphere, 12(6), 694, doi: 10.3390/atmos12060694, 2021.

Vecchiato, M., Barbaro, E., Spolaor, A., Burgay, F., Barbante, C., Piazza, R. and Gambaro, A., Fragrances and PAHs in snow and seawater of Ny-Ålesund (Svalbard): Local and long-range contamination. Environmental Pollution 242, 1740-1747, doi: 10.1016/j.envpol.2018.07.095, 2018.

Weingartner, E., Saathoff, H., Schnaiter, M., Streit, N., Bitnar, B. and Baltensperger, U.: Absorption of light by soot particles: determination of the absorption coefficient by means of aethalometers, J. Aerosol Sci., 34(10), 1445–1463, doi:10.1016/S0021-8502(03)00359-8, 2003.

Wendl, I. A., Menking, J. A., Färber, R., Gysel, M., Kaspari, S. D., Laborde, M. J. G. and Schwikowski, M.: Optimized method for black carbon analysis in ice and snow using the Single Particle Soot Photometer, Atmospheric Meas. Tech., 7, 2667–2681, doi:10.5194/amt-7-2667-2014, 2014.

Xu, B., T. Yao, X. Liu, and N. Wang, Elemental and organic carbon measurements with a two-step heating gas chromatography system in snow samples from the Tibetan Plateau, Ann. Glaciol., 43, 257–262, doi: 10.3189/172756406781812122, 2006.

Yasunari, T. J., Tan, Q., Lau, K.-M., Bonasoni, P., Marinoni, A., Laj, P., Ménégoz, M., Takemura, T. and Chin, M.: Estimated range of black carbon dry deposition and the related snow albedo reduction over Himalayan glaciers during dry pre-monsoon periods, Atmos. Environ., 78, 259–267, doi:10.1016/j.atmosenv.2012.03.031, 2013.

Zanatta, M., Gysel, M., Bukowiecki, N., Müller, T., Weingartner, E., Areskoug, H., Fiebig, M., Yttri, K. E., Mihalopoulos, N., Kouvarakis, G., Beddows, D., Harrison, R. M., Cavalli, F., Putaud, J. P., Spindler, G., Wiedensohler, A., Alastuey, A., Pandolfi, M., Sellegri, K., Swietlicki, E., Jaffrezo, J. L., Baltensperger, U. and Laj, P.: A European aerosol phenomenology-5: Climatology of black carbon optical properties at 9 regional background sites across Europe, Atmos. Environ., 145, 346–364, doi:10.1016/j.atmosenv.2016.09.035, 2016.

Zanatta, M., Laj, P., Gysel, M., Baltensperger, U., Vratolis, S., Eleftheriadis, K., Kondo, Y., Dubuisson, P., Winiarek, V., Kazadzis, S., Tunved, P. and Jacobi, H.-W.: Effects of mixing state on optical and radiative properties of black carbon in the European Arctic, Atmospheric Chem. Phys., 18(19), 14037–14057, doi: 10.5194/acp-18-14037-2018, 2018.

Zangrando, R., Barbaro, E., Zennaro, P., Rossi, S., Kehrwald, N. M., Gabrieli, J., Barbante, C. and Gambaro, A.: Molecular Markers of Biomass Burning in Arctic Aerosols, Environ. Sci. Technol., 47(15), 8565–8574, doi:10.1021/es400125r, 2013.